Supplementary information (ESI)

SARS-CoV-2 Protein Monitored by Long-Range Surface Plasmon Field-Enhanced Raman Scattering with hybrid bowtie nanoaperture arrays and nanocavities

Xiaojun Luo,[a] Weiling Yue,[a] Shutong Zhang,[a] Haopeng Liu,[a] Zhinan Chen,[a] Ling Qiao,[b] Panjie Li,[c]* Caijun Wu[a]* Yi He [a]*

[a] *School of Science，Xihua University，Chengdu 610039，P. R. China*

[b] *Division of Chemistry and Biological Chemistry, School of Physical & Mathematical Sciences, Nanyang Technological University, Singapore 637371, Singapore*

[c] *School of Chemistry and Chemical Engineering, School of Environmental and Biological Engineering, Nanjing University of Science and Technology, Nanjing 210094, China*

Gene sequence of SARS-CoV-2 S protein

QCVNLTTRTQLPPAYTNSFTRGVYYPDKVFRSSVLHSTQDLFLPFFSNVTWFHAIHVSGTNGTK
RFDNPVLPFNDGVYFASTEKSNIIRGWIFGTTLDSKTQSLLIVNNATNVVIKVCEFQFCNDPFLG
VYYHKNNKSWMESEFRVYSSANNCTFEYVSQPFLMDLEGKQGNFKNLREFVFKNIDGYFKIYS
KHTPINLVRDLPQGFSALEPLVDLPIGINITRFQTLLALHRSYLTPGDSSSGWTAGAAAYYVGYL
QPRTFLLKYNENGTITDAVDCALDPLSETKCTLKSFTVEKGIYQTSNFRVQPTESIVRFPNITNLC
PFGEVFNATRFASVYAWNRKRISNCVADYSVLYNSASFSTFKCYGVSPTKLNDLCFTNVYADS
FVIRGDEVRQIAPGQTGKIADYNYKLPDDFTGCVIAWNSNNLDSKVGGNYNYLYRLFRKSNLK
PFERDISTEIYQAGSTPCNGVEGFNCYFPLQSYGFQPTNGVGYQPYRVVVLSFELLHAPATVCG
PKKSTNLVKNKCVNFNFNGLTGTGVLTESNKKFLPFQQFGRDIADTTDAVRDPQTLEILDITPCS
FGGVSVITPGTNTSNQVAVLYQDVNCTEVPVAIHADQLTPTWRVYSTGSNVFQTRAGCLIGAE
HVNNSYECDIPIGAGICASYQTQTNSPRRAR

Gene sequence of SARS-CoV-2 N protein

MSDNGPQNQRNAPRITFGGPSDSTGSNQNGERSGARSKQRRPQGLPNNTASWFTALTQHGKED
LKFPRGQGVPINTNSSPDDQIGYYRRATRRIRGGDGKMKDLSPRWYFYYLGTGPEAGLPYGAN
KDGIIWVATEGALNTPKDHIGTRNPANNAAIVLQPQGTTLPKGFYAEGSRGGSQASSRSSSRSR
NSSRNSTPGSSRGTSPARMAGNGGDAALALLLLDRLNQLESKMSGKGQQQQGQTVTKKSAAE
ASKKPRQKRTATKAYNVTQAFGRRGPEQTQGNFGDQELIRQGTDYKHWPQIAQFAPSASAFFG
MSRIGMEVTPSGTWLTYTGAIKLDDKDPNFKDQVILLNKHIDAYKTFPPTEPKKDKKKKADET
QALPQRQKKQQTVTLLPAADLDDFSKQLQQSMSSADSTQA

The calculation of the average distributed protein particles within the Raman-focused window

The irradiation radius (r) of focus laser beam can be described as:[1]

$$r = \frac{1.22\lambda}{2N.A.}$$

where, λ represents excitation wavelength. N.A is the numerical aperture of the objective. Thus, the r of focus laser beam in our system is ~0.5 μm.

Because 100 μL SARS-CoV-2 proteins were uniform distributed on 1× 1 cm^2 substrate surface, the effective number of proteins (*N*) within Raman-focused window can be calculated as follow: [2]

$$N = \frac{C\ g/mL}{Mw\ g/mol} \times 0.1\ mL \times \frac{3.14 \times 0.5\ \mu m \times 0.5\ \mu m}{1000\ \mu m \times 1000\ \mu m} \times NA$$

The Mw (molecular weight) of S protein is 180 kDa (1.8×10^5 g/mol). NA (Avogadro constant) is 6.02×10^{23} mol^{-1}.

[1] R. A. A´lvarez-Puebla, *J. Phys. Chem. Lett.*, 2012, **3**, 857−866.

[2] Y. Yang, Y. Peng, C. Lin, L. Long, J. Hu, J. He, H. Zeng, Z. Huang, Z.-Y. Li, M. Tanemura, J. Shi, J. R. Lombardi and X. Luo, *Nano-Micro Lett.*, 2021, **13**, 109.

Table S1. **Raman bands of typical vibrational modes of S protein**

Raman bands (cm^{-1})	Major Assignments
640	Tyr (α-helix)
708	Phospholipids
740	Trp, C–C stretching
815	Tyr
860	Tyr
945	N–C_α–C
1045	C–N and C–C protein stretching
1146	Gly
1170	Tyr
1262	α-helix amide III
1325	α-helix amide III
1358	C–H deformation, Trp
1400	C–H rocking in lipids
1450	General fatty acids, C–H stretching of glycoproteins
1565	Indole ring (Trp)
1610	Tyr, Trp, Phe

Table S2. **Raman bands of typical vibrational modes of N protein**

Raman bands (cm^{-1})	Major Assignments
640	Tyr (α-helix)
708	Phospholipids
740	Trp, C–C stretching
815	Tyr
860	β-Sheet Tyr
1045	C–N and C–C protein stretching
1262	Amide III
1358	C–H deformation, Trp
1400	C–H rocking in lipids
1450	General fatty acids, C–H stretching of glycoproteins
1565	Indole ring (Trp)
1660	Amide I

Table S3. **Raman bands of typical vibrational modes saliva sample**

Raman bands (cm^{-1})	Major Assignments
845	Ring breathing mode of tyrosine and C–C stretch of proline ring
923	C–C stretching of proline ring/glucose/lactic acid
1130	C–C stretching of proteins and lipids
1230	Amide III
1279	Amide III, Phospholipid, proteins, lipids
1360	Trp, porphyrins, lipids, proteins
1434	CH_2 deformation of proteins and lipids
1534	Trp
1640	CH_2 bending of Amide I and proteins

Figures

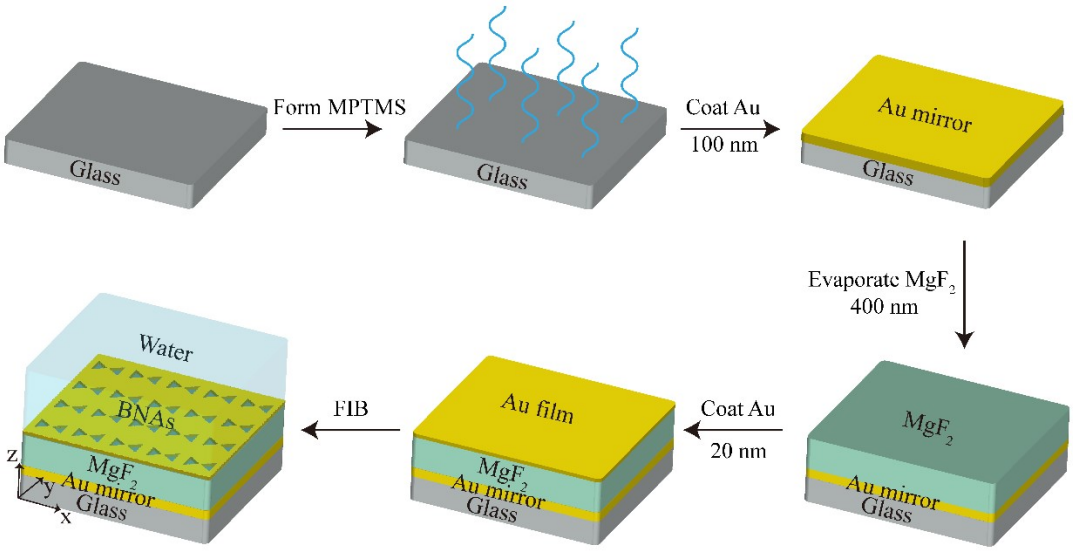

Fig. S1. Schematic illustration for the fabrication of BNAs + IMI + MIM substrates.

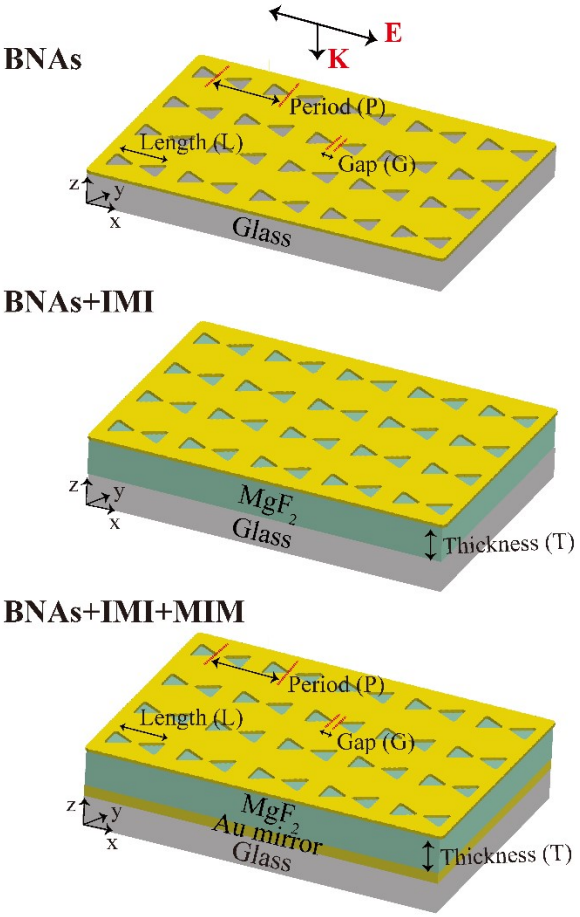

Fig. S2. 3D schematics for the three types of SERS substrates investigated in the FDTD simulations.

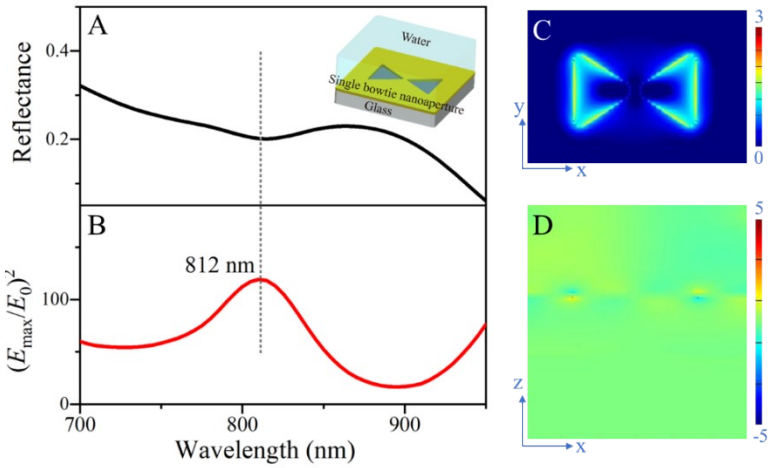

Fig. S3. (A) FDTD simulated reflectance and (B) $(E_{max}/E_0)^2$ intensity at the top Au/H_2O interface as a function of waveSlength for a single bowie nanoaperture. (C and D) The *E*-field profile at the top Au/water interface and *Ez* distribution at the cross-sectional x−z plane at the wavelength of 812 nm. The scale bar in C represents $(E_{max}/E_0)^2$ on a log scale. The scale bar in D represents $|E_z/E_0|$ on the normal scale.

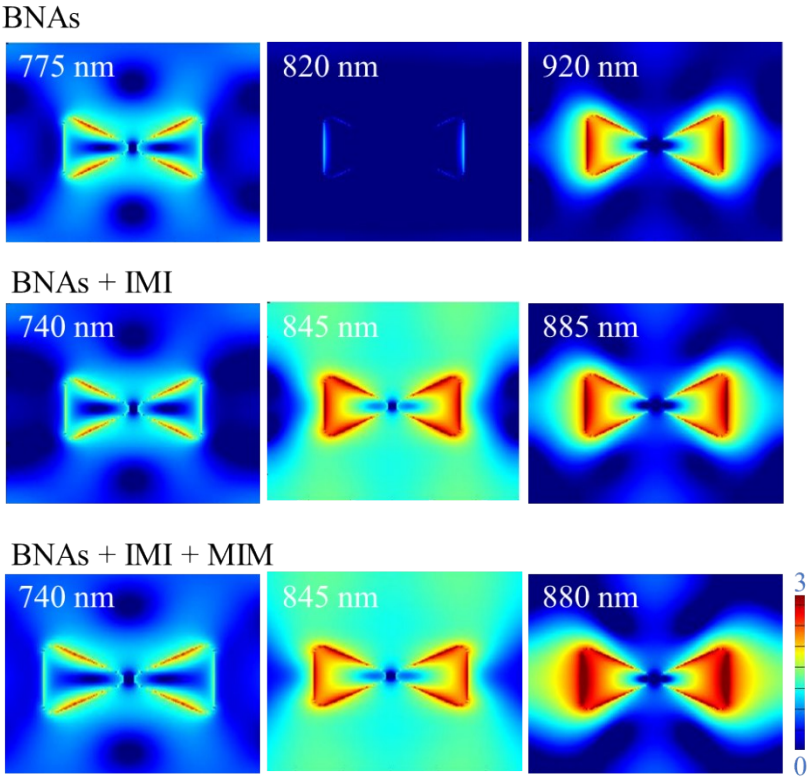

Fig. S4. FDTD simulated *E*-field distribution profiles for the three types of SERS substrates at the top Au/water interface at different resonance wavelength. The scale bar represents $(E_{max}/E_0)^2$ on a log scale.

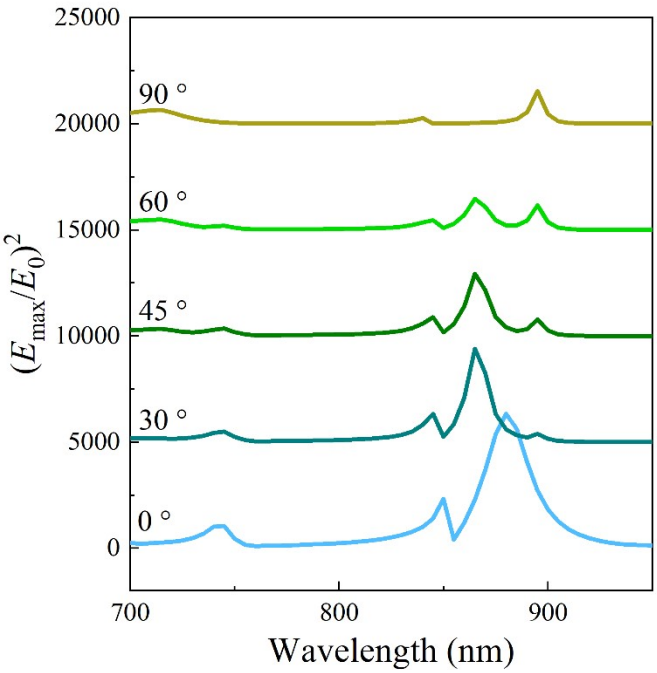

Fig. S5. FDTD simulated $(E_{max}/E_0)^2$ at the top Au/H_2O interface as a function of wavelength for BNAs + IMI + MIM structure at different polarization directions.

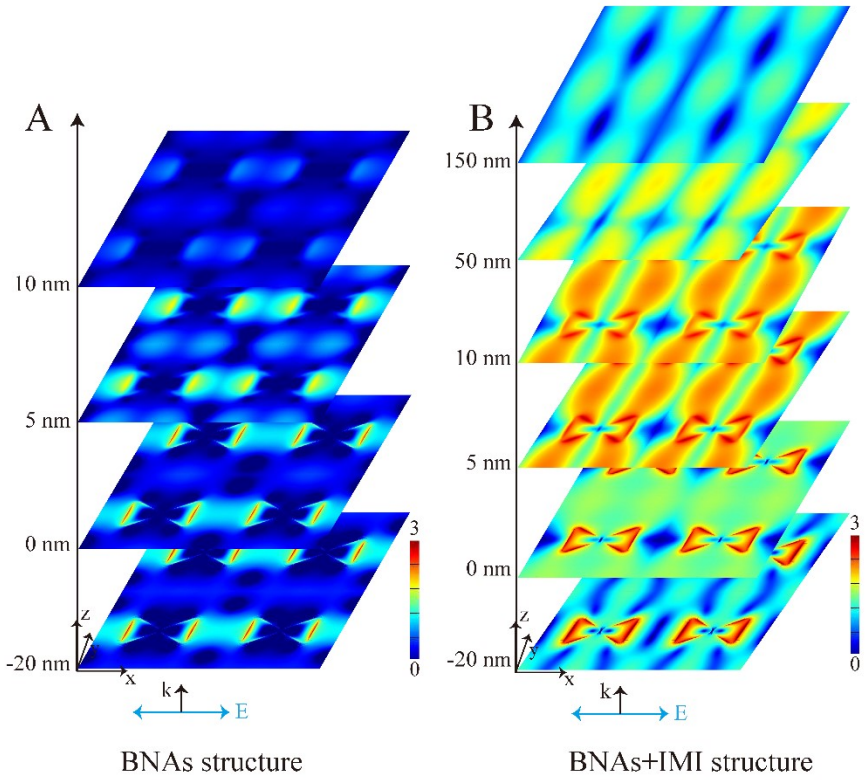

Fig. S6. FDTD simulated *E*-field distribution of x−y plane at different vertical distance from the top surface at mode III of (A) BNAs, (B) BNAs + IMI structure.

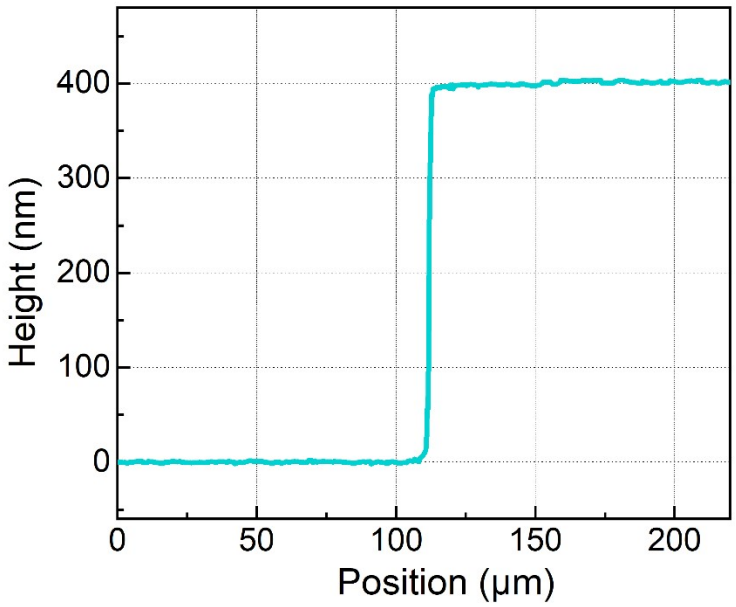

Fig. S7. Profilometer of MgF_2 thickness.

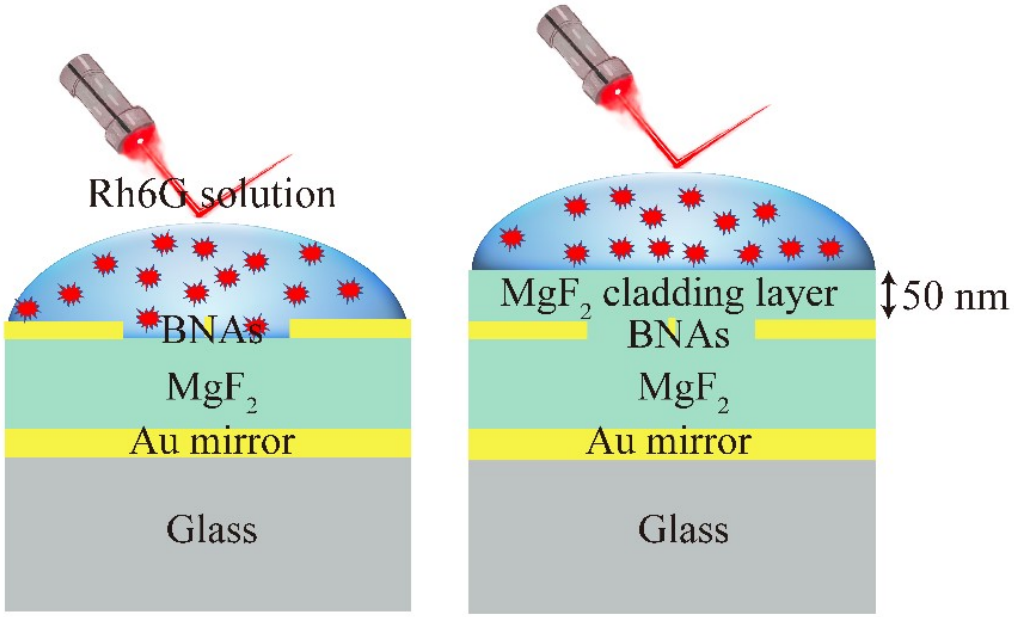

Fig. S8. Schematic illustration of Rh6G absorbed on the surface of the top Au/water interface (left) and absorbed on MgF_2/water interface with a MgF_2 capping layer thickness of 50 nm (right).